Clayey-Silty Sediments Containing Gas Hydrate in South China Sea: Geophysical and Geomechanical Results

Shi Shen[1,*], Rui Qin[2,3], Haihong Chen[2,3], Ting Huang[2,3], Yang Ge[2,3], Xin Lv[1], Huiyong Liang[1]

[1]Ningbo Institute of Dalian University of Technology, Ningbo, 315016, China
[2]State Key Laboratory of Offshore Natural Gas Hydrates, Beijing, 100028, China
[3]China National Offshore Oil Corporation Research Institute Co. LTD, Beijing, 100028, China

*shenshi_nbi@dlut.edu.cn

Abstract. Huge gas hydrate reserves exist worldwide, and over 90% of them occur in fine-grained reservoirs with poor permeability, such as the hydrate reservoir in the South China Sea (SCS). This type of hydrate reservoir is characterized by non-diagenesis and weak cementation, and hydrate exploitation is prone to trigger reservoir settlement and deformation. Therefore, the key to achieving the safe exploitation of hydrate resources is to conduct in-depth research into the geophysical and geomechanical features of hydrate-bearing sediments (HBSs) in the SCS. Based on this, the geophysical and geomechanical characteristics of the hydrate reservoirs in the Shenhu area of the SCS were thoroughly researched in this work. For the geophysical properties of HBSs, the host sediments of SCS belong to well-graded clayey silts, with particles arranged in a layered configuration face-to-face. Its principal mineral components include quartz, plagioclase, calcite and some clay minerals. For the geomechanical properties of HBSs, the strength, stiffness and volumetric strain of HBSs of SCS increase with effective confining pressure (ECP) under drained conditions. When the pore water is not emptied, the extra pressure is positive, demonstrating substantial shear contraction, and the fitting failure line is unaffected by the ECP. The aforementioned research contents can serve as a guide for future constitutive model and numerical simulation development on hydrate reservoir stability of SCS.

Keywords: Gas hydrates; clayey silts; South China Sea; Geophysical properties; Geomechanical properties.

1 Introduction

Natural gas hydrate (NGH) is a type of cage crystal that is widely distributed in permafrost areas and deep-sea sediments. It is made up of natural gas and water. Through multiple exploratory missions, the China Geological Survey (CGS) successfully drilled NGH cores in the Shenhu area of the South China Sea (SCS) in 2007, confirming the SCS's abundant reserves and broad development potential. In recent years, China has

H. Bilgin et al. (eds.), *Proceedings of the 2024 6th International Conference on Civil Engineering, Environment Resources and Energy Materials (CCESEM 2024)*, Advances in Engineering Research 253,
https://doi.org/10.2991/978-94-6463-606-2_50

boosted its research and development spending on NGH extraction. It has twice successfully test-mined NGH in the Shenhu Sea in the South China Sea, breaking numerous world records in terms of continuous exploitation time and production, which marks that China is steadily transitioning from experimental trial exploitation to commercial trial exploitation [26, 27].

Safety is a basic prerequisite for implementing the commercial exploitation of NGH in the SCS, which calls for extensive basic research accumulation and technological innovation [12, 25]. NGH reservoir in SCS is characterized by low permeability and fine grains, and hydrates are frequently present in the pore space of sediments in the form of patchy distribution. The aforementioned features determine that the fine-grained hydrate reservoir in the South China Sea has extremely complex mechanical properties [18, 25]. During the NGH mining process, the decomposition of NGH leads to the destruction of the original cemented structure, thereby weakening the bearing capacity of the deposits [13, 19, 22]; Additionally, a significant amount of gas produced by hydrate exploitation and decomposition will alter the stress state of the reservoir, result in reservoir deformation, and even lead to offshore engineering structures instability, submarine landslides and other engineering geological disasters [5]. Therefore, prior to becoming aware of NGH's commercial exploitation in the SCS, it is imperative to completely understand the geomechanical properties of the fine-grained hydrate reservoir in the SCS.

To look at the hydrate-bearing sediments' (HBSs') geomechanical characteristics in the SCS, various techniques have been used to carry out pertinent experimental research. Certain scholars adopted “mixed sample preparation method” to examine HBSs's mechanical characteristics in the SCS. They discovered that the stress-strain and strength characteristics of HBSs in the SCS are essentially identical to those of kaolin clay containing hydrates, indicating that kaolin can be used to replace marine soils of SCS, which are difficult to obtain to investigate the mechanical properties of hydrate reservoirs in the SCS (Luo et al., 2016, Kuang et al., 2019, Wang et al., 2017, Wang et al., 2019, Li et al., 2019) [6, 7, 11, 14, 17]. However, this approach has the following drawbacks for analyzing the mechanical characteristics of the submarine hydrate reservoir in SCS: (1) Since the temperature of submarine hydrate reservoir is typically over 273K and the test temperature for hydrate-bearing samples manufactured using this approach is below 273K, this method is not suited to submarine hydrate reservoir; (2) The hydrates are mixed with ice powder in this approach, which does not take into account how pore pressure affects the mechanical characteristics of HBSs; (3) This method does not consider the influence of hydrate nucleation location and non-uniformity distribution on strength and deformation characteristics. In order to solve the aforementioned issues, some researchers started attempting to implement the "partial water saturation approach" to generate hydrates and examine the mechanical properties of HBSs of SCS. To maximize the effectiveness of the experiments, Li et al. attempted to explore the SCS's HBSs' deformation properties and strength through multistage triaxial loading [9]. The study demonstrates that only under low effective stress levels can the stress-strain and volumetric strain curves of HBSs be very constant. Wang et al. thoroughly examined the influence of saturation of hydrates on the strength characteristics of HBSs in the SCS and confirmed that it will enhance the strength, modulus,

cohesion and angle of internal friction in sediments [15]. Wu et al. applied this method to examine the microstructure and HBSs's mechanical properties in the SCS [23, 24]. The findings demonstrate that hydrates in the pores are primarily present in the accumulation habits of patchy cluster. Additionally, if the over consolidation ratio rises, the strength and stiffness of HBSs of SCS will improve, and the strain-softening properties will decrease. Although the in-situ hydrate generation method is applied in the above research, hydrates are in a gas saturated environment. The foregoing research, however, does not take into account the pore water effects on sediment suction because the majority of submarine hydrate reservoirs occur in environments that are water saturated. Considering this, Wang et al. and Li et al. investigated the undrained mechanical properties of water saturated HBSs in the SCS [8, 20]. The conclusions demonstrated that the surplus pore water pressure is positive during shearing, and that the samples under an undrained condition are more likely to yield and approach the critical state than those under a drained condition.

Before investigating the geomechanical response of submarine hydrate reservoirs in SCS, it is crucial to examine the geophysical properties of HBSs for the following reasons: First, the geophysical properties determine the mechanical characterization of seafloor hydrate reservoir. Specific surface area, particle size distribution, liquid plastic limit and mineral composition are the primary variables determining the geomechanical properties of HBSs [16]. Secondly, it is challenging to obtain the undisturbed core samples due to the limited exploration projects, harsh sampling conditions, high economic costs, and a single follow-up detection method. Therefore, researchers often remold the core sample in the laboratory to replace the undisturbed core sample for mechanical experimental research. Knowing the geophysical properties of the HBSs has important guiding significance when remolding the core sample in the lab. In addition, when using the numerical simulators to predict and evaluate the gas production efficiency of the submarine hydrate extraction and the stability of the HBSs, the geophysical properties of the HBSs are also required input parameters to improve the accuracy of the numerical simulation. Therefore, it is of great practical importance to understand the geophysical properties of HBSs.

Based on the aforementioned contents, this paper conducts an in-depth analysis of the geophysical and geomechanical properties of HBSs in Shenhu Sea of SCS. For geophysical properties, we studied the particular surface area, liquid and plastic limits, mineral and element composition, and the grading of particle and pore size of sediment skeleton of HBSs in the SCS; For geomechanical properties, based on the sediment skeleton of the HBSs of the SCS, we generate 30% ~ 40% saturation of hydrates in its pores using partial water saturation method, and then carried out consolidation, drained shear and undrained shear tests in turn to study the strength and deformation properties of HBSs of the SCS.

2 Geophysical Properties of HBSs

The coring samples studied in this paper come from the Shenhu area in the SCS and are buried 2-3m below the seabed. They are provided by China National Offshore Oil

Corporation, depicted in Fig. 1. This section focuses on the geophysical properties of the host sediments of HBSs in the SCS, including particle size distribution, specific surface area, pore size distribution, liquid and plastic limits, mineral and element composition.

Fig. 1. Coring samples of the SCS

2.1 Experimental Apparatus and Methods

According to previous studies, the particle size of host sediments of the SCS is smaller than 5mm, so we utilize the "pyknometer method" to determine the specific gravity of host sediments in the SCS. A laser particle size analyzer was used to determine the host sediments' particle size distribution (Model: BT-9300ST, Baite Particle Size Instrument), shown in Fig. 2(a). The experimental method is as follows: Disperse about 0.5g of host sediments in 1000mL sodium hexametaphosphate-containing water, thoroughly stir it with a glass rod for about 1 minute, and the particle size distribution was measured with a laser particle size analyzer. For improved the measurement accuracy, the background calibration data of each test must be managed between 1 and 6, and the shading rate must be adjusted at roughly 20% each time.

The specific surface area and pore size distribution of host sediments are determined by the specific surface area and pore size analyzer (Beijing Jingwei Gaobo Science and Technology Co., Ltd., model: JW-BK222), which nitrogen adsorption and desorption experiments were carried out on host sediments at 77 K and static volumetric method was used [1]. The apparatus used are shown in Fig. 2(b). Morphological characteristics of the sediments were obtained using high-resolution field emission scanning electron microscopy (SEM) in vacuum mode, and the equipment used are shown in Fig. 2(c).

The liquid-plastic combination tester establishes the host sediments' liquid and plastic limitations, depicted in Fig. 2(d). First, measure the sinking depth of 76g cone in host sediments under three different water contents, and then draw a double logarithmic coordinate relationship curve with the water content of marine soil as the abscissa and the sinking depth of cone as the ordinate. According to the relation curve established, the water content of the cone when it dips 17 mm and 2 mm in the host sediments are the liquid and plastic limit, respectively.

The mineral composition of host sediments of the SCS was determined by X-ray diffraction (XRD), shown in Fig. 2(e). The SCS's host sediments' metal element compositions were ascertained using an inductively coupled plasma (ICP) spectrometer, present in Fig. 2(f).

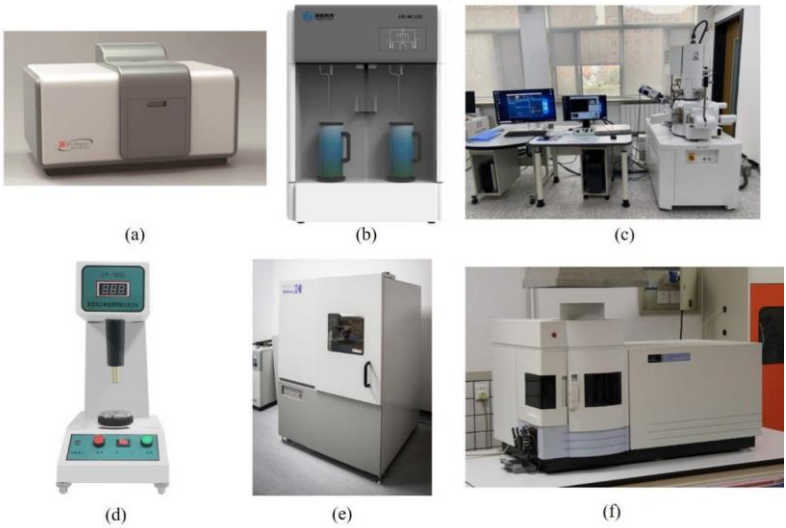

Fig. 2. Experimental apparatus: (a) Laser particle size analyzer; (b) Specific surface area and pore size analyzer; (c) Field Emission Scanning Electron Microscope; (d) liquid-plastic combine tester; (e) X-ray diffraction; (f) inductively coupled Plasma spectrometer

2.2 Geophysical Properties

The mineral concentration, organic matter content, and organic-inorganic composite colloid (the weighted average specific gravity of these components) all affect the specific gravity of soil particles. About 2.73g/cm^3 is the specific gravity of the host sediments, which is comparable to other measurements of the specific gravity of marine soils in the SCS [6]. Particle size distribution, which is directly related to the engineering properties of soil such as water permeability, compactness, and strength, describes the relative fraction of each type of particle in the soil and may be used to efficiently illustrate the homogeneity and continuity of soils. Fig. 3 (a)shows the host sediments' particle size distribution in the SCS under study in this publication. The mean grain size d50 of host sediments is 9.810 μm, and grain size is mostly between 0.1 and 64 μm. As described in Table. 1, there are 25.04% of particles smaller than 4um (clay) is, 75.92% of particles between 4 μm and 64 μm (silt) is, and 0.06% of particles greater than 63 μm. The content of fine-grained soils (clay and silt) is more than 99%, which gives the soil particles a larger ability to absorb combined water, as shown by a higher plasticity index and a lower permeability coefficient. By plotting the above data in the sediment three-phase diagram (Fig. 3(b)), it can be concluded that the host sediments in the SCS studied in this paper belong to clayey silts.

Table. 1 also provides the information of characteristic particle sizes (d10, d30, d50 and d60), and calculates the corresponding uniformity and curvature coefficients. Calculations reveal that the uniformity coefficient Cu ≥ 5 (uneven soil grading), and the curvature coefficient Cc range between 1-3 (continuous grading curve). Hence, the marine soils of the SCS studied in this paper can be considered well-graded clayey silts.

The structural characteristics are the fundamental conditions for determining the engineering geological properties of HBSs. It is a crucial foundation for understanding the origins of soils since it frequently reflects the type of transport medium and the characteristics of sedimentary environment. SEM analysis of the host sediments in the top left corner of Fig. 3(a) reveals that most particles are organized edge to edge or edge to surface, resulting in flocculation and alveolate structure.

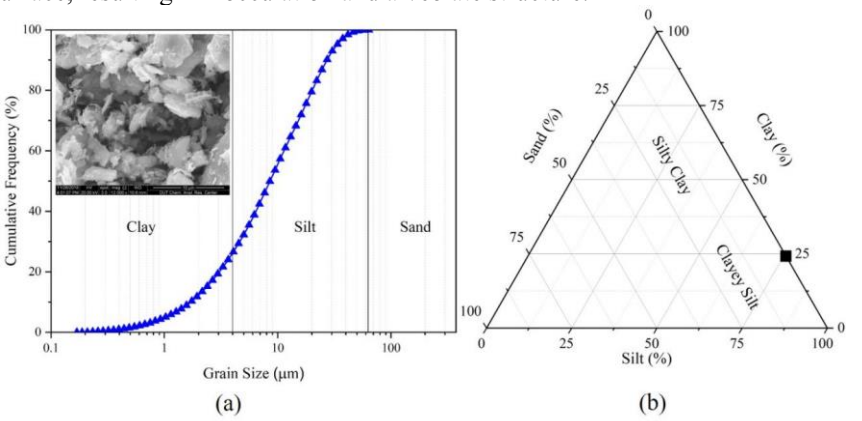

Fig. 3. Grain size distribution curve and three-phase map of the host sediments of SCS

Table 1. Geophysical propeties of the host sediments in the SCS

	Type	Value
	specific gravity (g/cm^3)	2.73
	specific surface area (m^2/g)	21.83
Fraction [weight]	Clay: 0~4μm (%)	24.02
	Silt: 4~63μm (%)	75.92
	Sand: >63μm (%)	0.06
Particle size parameter	d_{10} (μm)	1.896
	d_{30} (μm)	5.208
	d_{50} (μm)	9.810
	d_{60} (μm)	13.082
	C_u	6.900
	C_c	1.094
Liquid and plastic limits index	Water content w (%)	50.30
	Plastic limit w_P (%)	27.98
	Liquid limit w_L (%)	42.05
	Plasticity index I_P (%)	14.07
	Liquidity index I_L	1.585

Particle specific surface area is directly linked to permeability, rheology, and mechanical characteristics. As a result, the specific surface area test is crucial for examining the mechanical and physical characteristics of fine-grained soils. This research uses the dry method (gas absorption method) to determine the specific surface area and pore size distribution of soil. The specific surface area Sa is 21.83 m2/g, and the isotherm adsorption and desorption curves are H3 type hysteresis curves as shown in Fig. 4, indicating that the particle shape of marine soils is predominantly plate shaped, and most pores are of the fracture kind. In the upper left corner of Figure 4, the pore size distribution curve of the host sediments is depicted. The figure shows that the range of the pore size is primarily distributed between 2 and 10 nanometers (mesoporous).

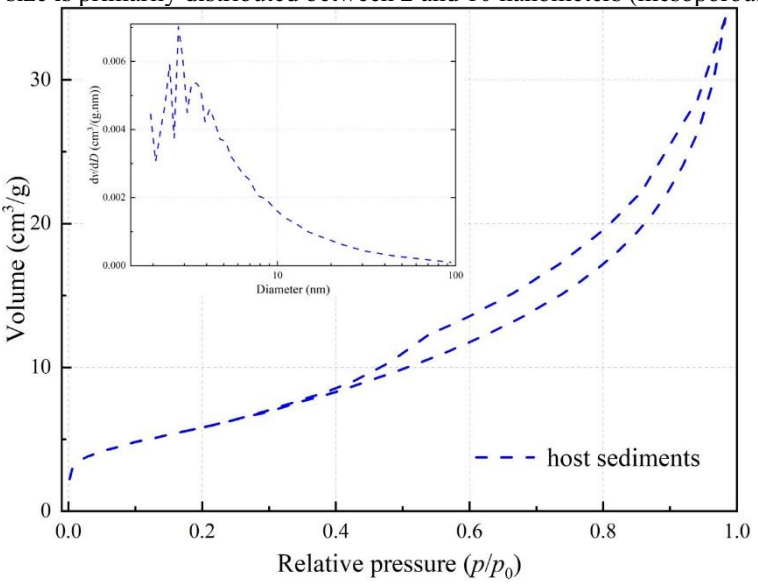

Fig. 4. Isothermal desorption and pore size distribution curves of the host sediments of SCS

Liquid and plastic limits are important water content limit indicators reflecting the various soft and hard states of fine-grained soil. The plastic limit and liquid limit of host sediments investigated in this paper are wp=27.98% and wL=42.05%, respectively, as shown in Table. 1 and Fig. 5. The water content (50.30%) is greater than the liquid limit. According to the classification of the soft and hard states of the cohesive soil, the soil is determined to have important rheological characteristics and to be in the flow plastic state. The plasticity index is usually used as the basis for the classification of fine-grained soils. Additionally, it indicates the maximum range of fine-grained soil's water content variation while it is plastic. That is, the higher the plasticity index, the more bound water is adsorbed. Through calculation, the plastic index IP (IP= wL - wp) and liquid index IL (IL= (w - wp)/(wL - wp)) of marine soil are 14.07 and 1.585, respectively. By putting the liquid limit wL and plasticity index IP data of host sediments on the plastic map, it is discovered that they fall into the category of medium compressibility.

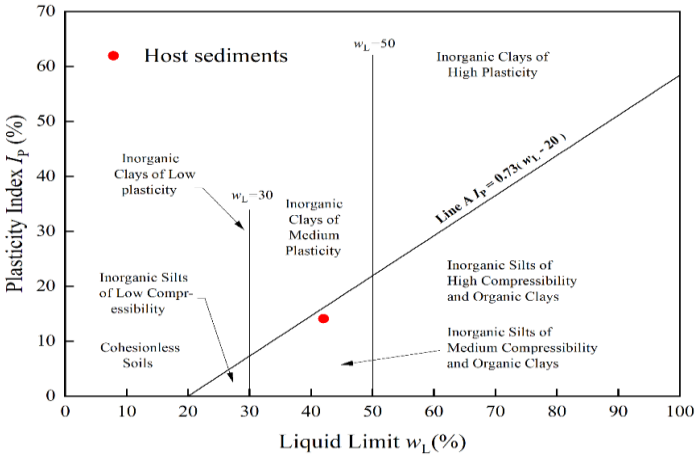

Fig. 5. Plasticity index I_p versus liquid limit w_L

Mineral composition occupies a crucial position in determining both the physical and technical qualities of soil as well as its regional difference. By using XRD to identify the various mineral compositions in the host sediments, the contents of each component were quantitatively assessed in accordance with the intensity and half-width of the diffraction peak. The XRD tests demonstrate that the host sediments mostly consist of quartz, calcite and plagioclase as shown in Fig.6 and Table. 2, which together make up 32.7%, 20.9% and 12.4% of the total, while illite and kaolinite accounting for 41% and 12% of the clay mineral, respectively. Illite can exist in environments that are neutral, slightly acidic, or alkaline. Kaolinite has a limited capacity to absorb bound water due to the low activity index and adsorption capacity. Simultaneously, the distribution of Ca, Na, Al, K, Fe, C, S and N in soils was also determined. Among metal elements, the content of Ca is the highest (except for Si), and the content of active elements K and Na is generally high. As indicated in Table. 2, the highest concentration of non-metallic elements is C.

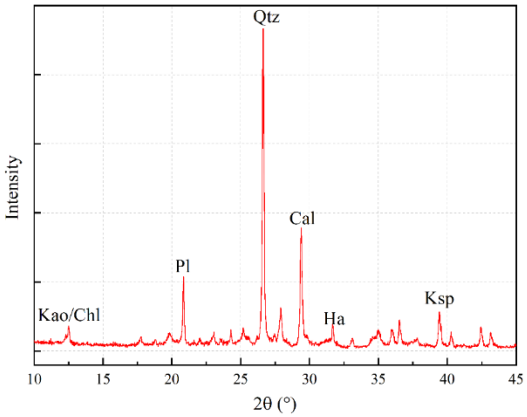

Fig. 6. XRD results of the host sediments of SCS

Table 2. Mineral and element compositions of the host sediments in the SCS

	Type	Relative content
Total rock	Quartz	32.7
	K-feldspar	2
	Plagioclase	12.4
	Halite	1.4
	Calcite	20.9
	Pyrite	1.6
	Aragonite	1.8
	Clays	27.1
clay minerals	Illite	41
	Kaolinite	12
	Chlorite	19
	I/S	29
	Mixed-layer ratio %	63
Metallic element	Ca	0.5808
	Na	0.5220
	Al	0.4865
	K	0.3143
	Fe	0.2340
Non-metallic element	C	4.119
	S	0.326
	N	0.309

3 Geomechanical Properties of HBSs

3.1 Experimental Apparatus and Methods

In this paper, consolidation, drained and undrained shear tests are carried out by two sets of hydrate triaxial apparatus as show in Fig. 7 (Fig. 7(a) for consolidation and drained triaxial tests; Fig. 7(b) for undrained triaxial tests). The pressure chamber, gas supply system, axial pressure control system, confined pressure control system, low temperature water bath system, and data collecting system are the main components of the two experimental apparatuses.

The pressure chamber offers a high-pressure sealing environment for hydrate generation. The confining pressure control system is mainly controlled by the confining pressure pump so that the hydraulic pressure can automatically adjust with pore pressure to maintain the effective confining pressure (ECP) constant during the reaction process. Axial pressure control system applies axial pressure through axial pressure pump to perform triaxial shear on soils. The low temperature water bath system uses ethylene glycol water solution as coolant. The data acquisition system consists of several pressure sensors, temperature sensors, collectors, and computer terminals, which can track real-time changes of parameters in reaction process.

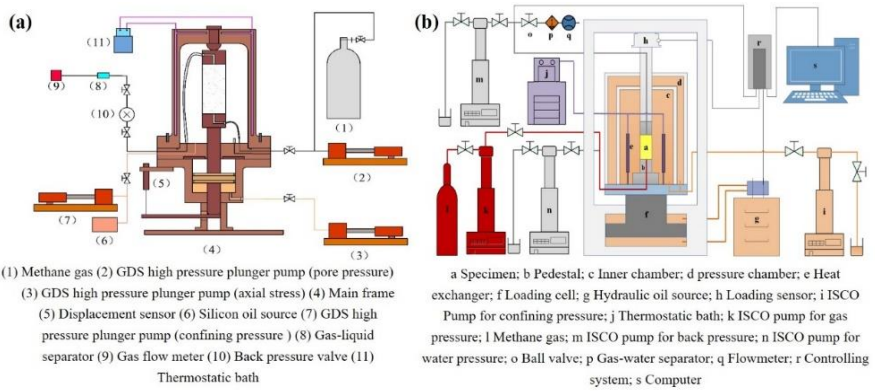

Fig. 7. Hydrate triaxial apparatus: (a) for consolidation and drained triaxial tests; (b) for undrained triaxial tests

HBSs are sampled by partial water saturation method, and the specific steps can be detailed in our previous articles. After hydrate-bearing sample preparation, isotropic loading and unloading test (consolidation test), consolidated drained triaxial tests and consolidated undrained triaxial tests are conducted, respectively. For isotropic loading and unloading test, the mean effective stress is gradually increased from 0.1MPa to 10MPa, and then unloaded from 10MPa to 3MPa. During the experiment, the void ratio of the sample had to be stabilized for more than 12 hours at each pressure level, and the variation of void ratio during the consolidation process was recorded. For consolidated drained (CD) triaxial tests, adjust the sample pore pressure and temperature to the target value (Table. 3 for details). Thereafter, isotropic consolidation is carried out under the target ECP. When the sample volume practically stays the same, the consolidation process is deemed to be completed. Lastly, under drained conditions, triaxial drained shear tests were performed at a constant strain rate of 0.1%/min. Close the drain valve during shearing for consolidated undrained (CU) triaxial testing, with a strain rate of 0.04%. Observe how axial strain affects the deviator stress and pore pressure.

Table 3. Geomechanical test conditions of the HBSs in the SCS

Case	Temperature (℃)	Pore pressure (MPa)	Hydrate saturation (%)	ECP (MPa)	Strain rate (%/min)	Remarks
1	0.5	6	32.7	0.1-10-3	-	Consolidation test
2			41.14	0.5		
3	0.5	12	38.49	1	0.1	Consolidated drained tests
4			40.36	2		
5			28.7	1		
6	8	12	30.4	2	0.04	Consolidated undrained tests
7			29.8	3		

3.2 Stress-Void Ratio Response

Accurate calculation of the compression deformation of HBSs is one of the core issues for the safe hydrate exploitation [4, 28]. Therefore, it is necessary to carry out research on the compression tests of HBSs in the SCS. In this section, we carried out isotropic loading and unloading experiments on HBSs to obtain the normal consolidation and over-consolidation lines and calculate the compression and swelling indexes.

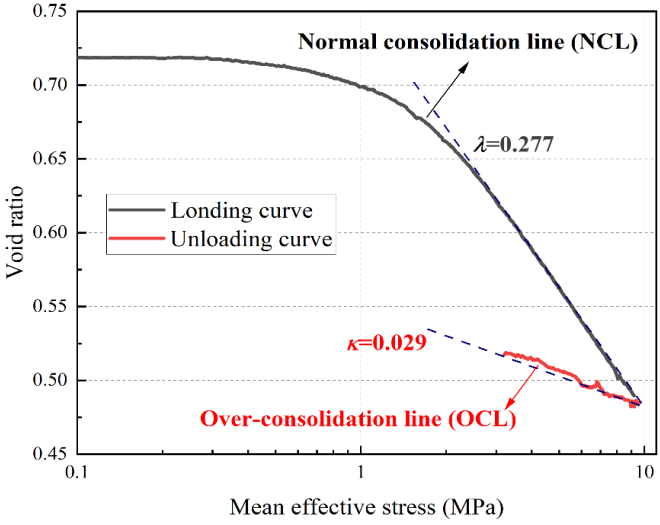

Fig. 8. Stress-void ratio response of HBSs in the SCS

As depicted in Fig. 8, the compression curve of HBSs exhibits obvious nonlinearity. The initial section of the HBSs' compression curve is very gentle. When the mean effective stress surpasses a specific point (1~2 MPa), there is a steep drop section, which is different from that of the nonstructural soil. This is primarily due to the fact that, when the HBSs' structure (hydrate-soil particle/ particle-particle function) is undamaged, the structure has a certain role in reducing the soil compression. While the HBSs' structure is destroyed, due to the altered internal connection state of the soil, The impact of soil structure on the compressibility gradually disappears as consolidation pressure is increased further, eventually becoming consistent with the compressibility of the hydrate-free sediments. Through calculation, the compression index of HBSs of SCS λ is 0.277, and the swelling index κ is 0.029, providing basic data for the formulation of the crucial state constitutive model of HBSs within the SCS.

3.3 Drained Triaxial Test

The drained mechanical properties of HBSs of SCS play an important role in assessing its long-term deformation characteristics. The following results can be analyzed from the stress-strain and volumetric strain curves of HBSs in the SCS at various ECP in Fig. 9: 1) The strain softening and shear expansion characteristics of HBSs are inhibited by high ECP, as evidenced by the gradual changes in the volumetric strain curve from

shear contraction to shear contraction and the type of stress-strain curve from strain softening to strain hardening. The high ECP has obvious reinforcing and compression effects on the specimens, which precisely align the arrangement of soil particles and hydrates [2]. Besides, increasing ECP will break down the particles and limit their turnover, which will inhibit the dilatancy and result in the shear contraction.

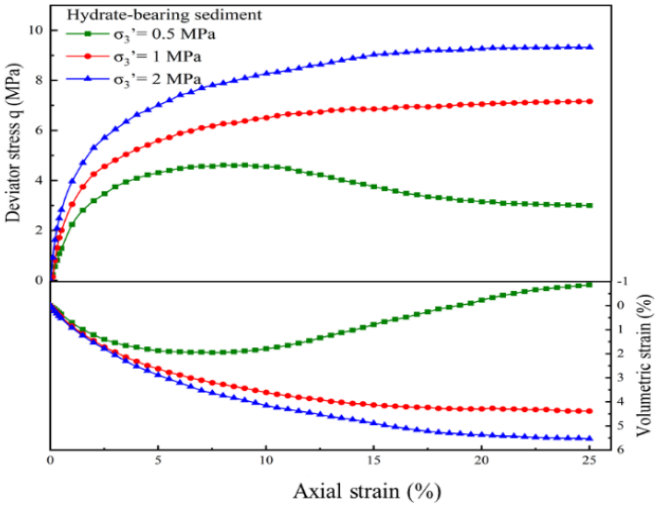

Fig. 9. Drained mechanical properties of HBSs of SCS: (a) stress-strain relationship; (b) volumetric strain curves

The strength, stiffness and volumetric strain of HBSs of SCS increase with the increase of ECP. The reason could be that as ECP increases, more constraints are placed on the HBSs, causing it to become more compact and less likely to generate and develop internal cracks. As a result, the HBSs become more resistant to deformation and have a higher failure strength and stiffness [3, 20]. Additionally, as ECP rises, fine particles find it easier to penetrate the pore spaces created by large particles, which makes it easier to be compressed for HBSs and increase the related volumetric strain.

3.4 Undrained Triaxial Test

Because of the fine-grained particles and low permeability of HBSs in the SCS, it is challenging for the internal pore fluid to be discharged when the submarine reservoir is compressed or sheared, which will result in the redistribution of pore pressure and effective stress in the sediments. In addition, the depressurization exploitation process will cause reservoir volume compression and a further decrease in permeability, making it more challenging to release pore fluid. Therefore, exploring the undrained mechanical properties of HBSs in the SCS is beneficial to the safe hydrate exploitation. Under the initial ECPs of 1, 2 and 3MPa, the relationships between the deviator stress q and axial strain ε_1, excess pore pressure u and ε_1, and q and mean effective stress p' of HBSs are compared, as displayed in Fig. 10. It can be observed from Fig. 10a) that the stress-strain relationships of different initial ECPs exhibit a clear strain hardening

feature. The reason is that fine-grained soils have smaller particles and a thicker surface water film than sand, which effectively lowers friction between the particles and makes the soil particles more easily filled into the pores [10, 15, 21]. This behavior results in the sample is sheared with greater integrity and resistance to deformation. From Fig. 10b), the excess pore pressure is positive during the whole shearing process, demonstrating a strong shear contraction. From Fig. 10c), the geometry of undrained stress paths of HBSs under various initial ECPs is similar, and the slope of failure line is essentially independent of the three initial ECPs.

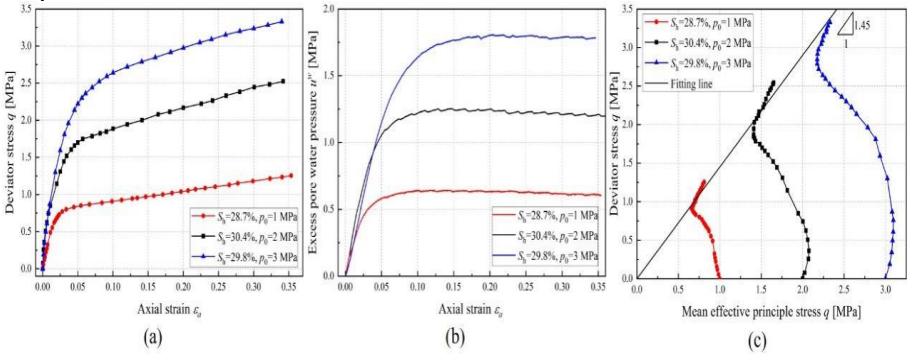

Fig. 10. Undrained mechanical properties of HBSs of SCS: (a) stress-strain relationship; (b) excess pore pressure curves; (c) effective stress paths

4 Conclusion

This paper systematically investigates the geophysical and geomechanical properties of HBSs in Shenhu Sea of SCS, including particle and pore size distribution, specific surface area, liquid and plastic limits, mineral and element composition, strength and deformation characteristics. The following conclusions are made considering the experimental findings:

(1) For geophysical properties, the host sediments of the SCS studied in this paper is well-graded clayey silts, and the particles are primarily orgnized edge to surface or edge to edge, resulting in flocculation and alveolate structure.

(2) For geomechanical properties, the compression index of HBSs of SCS λ is 0.277, and the swelling index κ is 0.029 of HBSs in the SCS. For CD triaxial tests, with an increase of ECP, the type of stress-strain curve gradually transits from strain softening to strain hardening, and the volumetric strain curve gradually changes from shear expansion to shear contraction. The strength, stiffness and volumetric strain of HBSs of SCS all increase as ECP increase. For undrained triaxial tests, the excess pore pressure is positive, and the failure line is almost independent of the initial ECP.

The research content of this paper can provide reference for the future constitutive model and numerical simulation work on reservoir stability of HBSs in the SCS.

Acknowledgement

This study was supported by the State Key Laboratory of Offshore Natural Gas Hydrates (2022-KFJJ-SHW), the Natural Science Foundation of Ningbo (2022J005).

Reference

1. Brunauner, S., Emmett, S. P. H. & Teller, E. 1938. Adsorption of gases in multimolecular layers. *Journal of the American Chemical Society,* 60**,** 309-319.
2. Dong, L., Li, Y., Liao, H., Liu, C., Chen, Q., Hu, G., Liu, L. & Meng, Q. 2020. Strength estimation for hydrate-bearing sediments based on triaxial shearing tests. *Journal of Petroleum Science and Engineering,* 184.
3. Ge, Y., Wang, L., Feng, K., Shen, S., Liu, Y., Wu, Z., Liu, Z. & Song, Y. 2024. High-pressure and temperature-controlled CPT calibration chamber based on deep-sea hydrate reservoirs. *Geoenergy Science and Engineering,* 242**,** 213207.
4. Kim, J., Dai, S., Jang, J., Waite, W. F., Collett, T. S. & Kumar, P. 2019. Compressibility and particle crushing of Krishna-Godavari Basin sediments from offshore India: Implications for gas production from deep-water gas hydrate deposits. *Marine and Petroleum Geology,* 108**,** 697-704.
5. Kim, Y.-G., Lee, S.-M., Jin, Y. K., Baranov, B., Obzhirov, A., Salomatin, A. & Shoji, H. 2013. The stability of gas hydrate field in the northeastern continental slope of Sakhalin Island, Sea of Okhotsk, as inferred from analysis of heat flow data and its implications for slope failures. *Marine and Petroleum Geology,* 45**,** 198-207.
6. Kuang, Y., Yang, L., Li, Q., Lv, X., Li, Y., Yu, B., Leng, S., Song, Y. & Zhao, J. 2019. Physical characteristic analysis of unconsolidated sediments containing gas hydrate recovered from the Shenhu Area of the South China sea. *Journal of Petroleum Science and Engineering,* 181.
7. Li, Y., Luo, T., Sun, X., Liu, W., Li, Q., Li, Y. & Song, Y. 2019. Strength Behaviors of Remolded Hydrate-Bearing Marine Sediments in Different Drilling Depths of the South China Sea. *Energies,* 12.
8. Li, Y., Wang, L., Shen, S., Liu, T., Zhao, J. & Sun, X. 2021a. Triaxial Tests on Water-Saturated Gas Hydrate-Bearing Fine-Grained Samples of the South China Sea under Different Drainage Conditions. *Energy & Fuels,* 35**,** 4118-4126.
9. Li, Y., Wu, D., Wu, P., Song, Y. & Sun, X. 2021b. Mechanical Characteristics of the Hydrate-Bearing Sediments in the South China Sea Using a Multistage Triaxial Loading Test. *Energy & Fuels,* 35**,** 4127–4137.
10. Liu, W., Liu, H., Wang, L., Feng, K., Shen, S., Liu, Y., Zhao, J. & Li, Y. 2024. Undrained Mechanical Properties of Overlying Soils of Gas Hydrate Reservoirs in the South China Sea. *Energy & Fuels***,** 3020-3031.
11. Luo, T., Song, Y., Zhu, Y., Liu, W., Liu, Y., Li, Y. & Wu, Z. 2016. Triaxial experiments on the mechanical properties of hydrate-bearing marine sediments of South China Sea. *Marine and Petroleum Geology,* 77**,** 507-514.
12. Ma, S., Liu, Z., Zheng, J.-N., Wu, Z., Li, N., Guan, X., Han, J.-N., Yang, M. & Song, Y. 2024. Natural Gas Hydrate Decomposition Characteristics at the Exploitation Anaphase via Sediment Warming. *Energy & Fuels,* 38**,** 14334-14342.
13. Shen, S., Sun, X., Wang, L., Song, Y. & Li, Y. 2021. Effect of Temperature on the Mechanical Properties of Hydrate-Bearing Sand under Different Confining Pressures. *Energy & Fuels,* 35**,** 4106-4117.

14. Wang, B., Huo, P., Luo, T., Fan, Z., Liu, F., Xiao, B., Yang, M., Zhao, J. & Song, Y. 2017. Analysis of the Physical Properties of Hydrate Sediments Recovered from the Pearl River Mouth Basin in the South China Sea: Preliminary Investigation for Gas Hydrate Exploitation. *Energies,* 10.
15. Wang, L., Li, Y., Shen, S., Liu, W., Sun, X., Liu, Y. & Zhao, J. 2022. Mechanical behaviours of gas-hydrate-bearing clayey sediments of the South China Sea. *Environmental Geotechnics,* 9**,** 210-222.
16. Wang, L., Li, Y., Wu, P., Shen, S., Liu, T., Leng, S., Chang, Y. & Zhao, J. 2020. Physical and mechanical properties of the overburden layer on gas hydrate-bearing sediments of the South China sea. *Journal of Petroleum Science and Engineering,* 189**,** 107020.
17. Wang, L., Liu, W., Li, Y., Wu, P. & Shen, S. 2019. Mechanical Behaviors of Methane Hydrate-Bearing Sediments Using Montmorillonite Clay. *Energy Procedia,* 158**,** 5281-5286.
18. Wang, L., Shen, S., Wu, Z., Chen, P. & Li, Y. 2023. Temperature Effect on Undrained Mechanical Properties of Hydrate-Bearing Clayey Silts in the South China Sea. *Energy & Fuels,* 37**,** 13025−13033.
19. Wang, L., Shen, S., Wu, Z., Wu, D. & Li, Y. 2024a. Strength and creep characteristics of methane hydrate-bearing clayey silts of the South China Sea. *Energy,* 294**,** 130789.
20. Wang, L., Sun, X., Shen, S., Wu, P., Liu, T., Liu, W., Zhao, J. & Li, Y. 2021a. Undrained triaxial tests on water-saturated methane hydrate–bearing clayey-silty sediments of the South China Sea. *Canadian Geotechnical Journal,* 58**,** 351-366.
21. Wang, L., Yu, W., Ge, Y., Shen, S., Wu, Z., Zhu, Y., Song, Y. & Li, Y. 2024b. Undrained triaxial tests of underconsolidated overlying sediments of hydrate deposits in the South China Sea. *Gas Science and Engineering,* 131**,** 205442.
22. Wang, L., Zhao, J., Sun, X., Wu, P., Shen, S., Liu, T. & Li, Y. 2021b. Comprehensive review of geomechanical constitutive models of gas hydrate-bearing sediments. *Journal of Natural Gas Science and Engineering,* 88**,** 103755.
23. Wu, P., Li, Y., Wang, L., Sun, X., Wu, D., He, Y., Li, Q. & Song, Y. 2022. Hydrate-bearing sediment of the South China Sea: Microstructure and mechanical characteristics. *Engineering Geology,* 307**,** 106782.
24. Wu, P., Li, Y., Wang, L., Wang, L., Sun, X., Liu, W. & Song, Y. 2021. Triaxial tests on the overconsolidated methane hydrate-bearing clayey-silty sediments. *Journal of Petroleum Science and Engineering,* 206**,** 109035.
25. Wu, Z., Gu, Q., Wang, L., Li, G., Shi, C., He, Y., Li, Q. & Li, Y. 2024. Experimental Study on Permeability and Gas Production Characteristics of Montmorillonite Hydrate Sediments Considering the Effective Stress and Gas Slippage Effect. *SPE Journal,* 29**,** 2525–2544.
26. Ye, J.-L., Qin, X.-W., Xie, W.-W., Lu, H.-L., Ma, B.-J., Qiu, H.-J., Liang, J.-Q., Lu, J.-A., Kuang, Z.-G., Lu, C., Liang, Q.-Y., Wei, S.-P., Yu, Y.-J., Liu, C.-S., Li, B., Shen, K.-X., Shi, H.-X., Lu, Q.-P., Li, J., Kou, B.-B., Song, G., Li, B., Zhang, H.-E., Lu, H.-F., Ma, C., Dong, Y.-F. & Bian, H. 2020. The second natural gas hydrate production test in the South China Sea. *China Geology,* 3**,** 197-209.
27. Ye, J., Qin, X., Qiu, H., Xie, W., Lu, H., Lu, C., Zhou, J., Liu, J., Yang, T., Cao, J. & Sa, R. 2018. Data Report: Molecular and Isotopic Compositions of the Extracted Gas from China's First Offshore Natural Gas Hydrate Production Test in South China Sea. *Energies,* 11.
28. Yoneda, J., Oshima, M., Kida, M., Kato, A., Konno, Y., Jin, Y. & Tenma, N. 2019. Consolidation and hardening behavior of hydrate-bearing pressure-core sediments recovered from the Krishna–Godavari Basin, offshore India. *Marine and Petroleum Geology,* 108**,** 512-523.